2016-09-28

Adipocyte-specific Hypoxia-inducible gene 2 promotes fat deposition and diet-induced insulin resistance

Marina DiStefano
University of Massachusetts Medical School

Et al.

Original Article

MOLECULAR METABOLISM

Adipocyte-specific Hypoxia-inducible gene 2 promotes fat deposition and diet-induced insulin resistance*

Marina T. DiStefano [1,4], Rachel J. Roth Flach [1,5], Ozlem Senol-Cosar [1,6], Laura V. Danai [1,7], Joseph V. Virbasius [1], Sarah M. Nicoloro [1], Juerg Straubhaar [1], Sezin Dagdeviren [2], Martin Wabitsch [3], Olga T. Gupta [1,8], Jason K. Kim [2], Michael P. Czech [1,*]

ABSTRACT

Objective: Adipose tissue relies on lipid droplet (LD) proteins in its role as a lipid-storing endocrine organ that controls whole body metabolism. Hypoxia-inducible Gene 2 (Hig2) is a recently identified LD-associated protein in hepatocytes that promotes hepatic lipid storage, but its role in the adipocyte had not been investigated. Here we tested the hypothesis that Hig2 localization to LDs in adipocytes promotes adipose tissue lipid deposition and systemic glucose homeostasis.

Method: White and brown adipocyte-deficient ($Hig2^{fl/fl}$ × Adiponection cre+) and selective brown/beige adipocyte-deficient ($Hig2^{fl/fl}$ × Ucp1 cre+) mice were generated to investigate the role of Hig2 in adipose depots. Additionally, we used multiple housing temperatures to investigate the role of active brown/beige adipocytes in this process.

Results: Hig2 localized to LDs in SGBS cells, a human adipocyte cell strain. Mice with adipocyte-specific Hig2 deficiency in all adipose depots demonstrated reduced visceral adipose tissue weight and increased glucose tolerance. This metabolic effect could be attributed to brown/beige adipocyte-specific Hig2 deficiency since $Hig2^{fl/fl}$ × Ucp1 cre+ mice displayed the same phenotype. Furthermore, when adipocyte-deficient Hig2 mice were moved to thermoneutral conditions in which non-shivering thermogenesis is deactivated, these improvements were abrogated and glucose intolerance ensued. Adipocyte-specific Hig2 deficient animals displayed no detectable changes in adipocyte lipolysis or energy expenditure, suggesting that Hig2 may not mediate these metabolic effects by restraining lipolysis in adipocytes.

Conclusions: We conclude that Hig2 localizes to LDs in adipocytes, promoting adipose tissue lipid deposition and that its selective deficiency in active brown/beige adipose tissue mediates improved glucose tolerance at 23 °C. Reversal of this phenotype at thermoneutrality in the absence of detectable changes in energy expenditure, adipose mass, or liver triglyceride suggests that Hig2 deficiency triggers a deleterious endocrine or neuroendocrine pathway emanating from brown/beige fat cells.

Keywords Obesity; Adipocyte; Lipid droplet; Lipolysis; Hypoxia-inducible gene 2 (Hig2)

1. INTRODUCTION

Once considered an inert storage organ, adipose tissue is now known to have numerous metabolic as well as endocrine functions with inputs into whole body metabolism [1]. Adipose tissue contains adipocytes, or fat cells, and preadipocytes, immune cells, and endothelial cells and stores the majority of caloric energy in the form of neutral lipids in adipocytes in organelles termed lipid droplets (LDs) [2,3]. LDs are

*This work was supported by the National Institutes of Health Grant: R37-DK030898 to M.P.C.

[1]From the Program in Molecular Medicine, University of Massachusetts Medical School, Worcester, MA 01605, USA [2]From the Program in Molecular Medicine and the Department of Medicine, Division of Endocrinology, Metabolism and Diabetes, University of Massachusetts Medical School, Worcester, MA 01605, USA [3]From the Division of Pediatric Endocrinology and Diabetes, Department of Pediatrics and Adolescent Medicine, University Medical Center Ulm, Ulm 89075, Germany

[4] Current address: Laboratory for Molecular Medicine, Partners HealthCare, Cambridge, MA, USA.
[5] Current address: Pfizer, Cambridge, MA, USA.
[6] Current address: Department of Pathology, Harvard Medical School, Boston, MA, USA.
[7] Current address: Koch Institute for Integrative Cancer Research, Massachusetts Institute of Technology, Cambridge, MA, USA.
[8] Current address: Department of Internal Medicine, Touchstone Diabetes Center, The University of Texas Southwestern Medical Center, Dallas, TX, USA.

*Corresponding author. Program in Molecular Medicine, University of Massachusetts Medical School, 373 Plantation Street, Worcester, MA, USA. Fax: +1 508 856 1617. E-mail: Michael.Czech@umassmed.edu (M.P. Czech).

Abbreviations: LD, lipid droplet; Hig2, Hypoxia-inducible gene 2; TG, triglyceride; FFA, free fatty acid; WAT, white adipose tissue; BAT, brown adipose tissue; Ucp1, uncoupling protein 1; HFD, high fat diet; SVF, stromal vascular fraction; SGBS, Simpson-Golabi-Behmel syndrome; eWAT, epididymal white adipose tissue; iWAT, inguinal white adipose tissue; ITT, insulin tolerance test; RER, respiratory exchange ratio; GTT, glucose tolerance test; NEFA, non-esterified fatty acid

Received September 7, 2016 • Revision received September 15, 2016 • Accepted September 19, 2016 • Available online 28 September 2016

http://dx.doi.org/10.1016/j.molmet.2016.09.009

highly dynamic organelles and are regulated by tissue-specific proteins embedded in or associated with the droplet termed LD proteins. These proteins can regulate LD size by inhibiting or facilitating lipolysis, the breakdown of triglycerides (TGs) into glycerol and free fatty acids (FFAs) [4]. LD proteins are relevant to human disease, as humans with mutations in these proteins manifest lipodystrophy, fatty liver, and metabolic syndrome [5].

Two main families of LD-associated proteins are the PAT family [6], named for its three founding members Perilipin, Adipophilin, and Tip47 which have PAT domains, and the CIDE family [7]. The PAT family has five members (Perilipin 1-5), while the CIDE family has three members (Cidea, Cideb, and Cidec/Fsp27). LDs are heterogeneous in terms of associated proteins and LD proteins generally demonstrate tissue-specific distribution patterns [8]. Perilipins 1, 2, 3, and 4, Cidea, and Fsp27 are expressed in adipose tissue and localize to LDs in adipocytes [6,9]. *In vitro* and *in vivo* studies suggest that Perilipin 1 and Fsp27 are two LD proteins that are critical for lipid storage in adipocytes [10–14]. These observations in cells and animal models were consistent with findings in lipodystrophic human subjects with Perilipin 1 and Fsp27 mutations [15,16].

In contrast to the major lipid storage function of white adipose tissue (WAT), brown adipose tissue (BAT) generates heat through non-shivering thermogenesis, or generation of heat by uncoupling of the proton gradient of the electron transport chain from ATP synthesis, mediated by uncoupling protein 1 (Ucp1) [17]. This differs from shivering thermogenesis, a temporary involuntary muscle movement that generates heat [18]. Brown adipocytes are characterized by high mitochondrial number, high Ucp1 expression, and small, numerous (multilocular) LDs [3]. Until recently, BAT was thought to be present solely for warmth in human infants and hibernating mammals, but 2FDG-PET scans have revealed that adult humans retain some functional BAT that can expand in response to cold exposure [19–21]. As BAT metabolism is energetically expensive, human BAT activation presents a unique anti-obesity therapeutic potential. BAT thermogenesis can be activated by many means, but one of the most prominent stimuli is increased beta-adrenergic activation in response to cold temperatures [17]. For example, when rodents are housed at room temperature (23 °C), a mild cold stress, their metabolic rate can increase up to 50% due to BAT energy consumption [22]. As housing mice at room temperature (23 °C) poses such a thermal stress, it can be informative to subject mouse models to thermoneutrality (30 °C for mice), the temperature at which they are not subject to external cold stress, to eliminate the contribution of nonshivering thermogenesis to whole body metabolism [23].

Hypoxia-inducible gene 2 (Hig2) is a 63 amino acid protein that we previously identified as a protein that localizes to LDs in hepatocytes and promotes hepatic lipid deposition by inhibiting lipolysis [24]. In this present study, we observed that Hig2 is highly expressed in the adipocyte fraction of adipose tissue samples collected from bariatric surgery patients, which in concert with its phenotype in hepatocytes prompted us to examine its role in adipose tissue. We demonstrate that Hig2 also localizes to LDs in adipocytes and its expression is increased with both adipogenic differentiation and fat deposition *in vitro*, suggesting that Hig2 may also play a role in adipose tissue *in vivo*. Mice harboring an adipocyte-specific deletion of Hig2 demonstrate reduced epididymal fat pad weight and improved glucose tolerance after high fat diet (HFD). These effects are abrogated by thermoneutral housing, suggesting that Hig2 may have an unexpected role in BAT in addition to WAT function. In support of this hypothesis, mice harboring a brown adipocyte-specific deletion of Hig2 also display improved glucose tolerance. Interestingly, *ex vivo* glycerol release, serum glycerol, and serum NEFAs are unchanged in adipocyte-specific Hig2-deficient animals compared with fl/fl controls, suggesting that Hig2 may use a lipolysis-independent mechanism to promote lipid deposition in adipocytes. Taken together, these results suggest that adipocyte-specific Hig2 promotes adipocyte lipid deposition and glucose intolerance, which may be entirely due to its control of BAT function *in vivo*.

2. MATERIALS AND METHODS

2.1. Animal studies

2.1.1. Breeding and genotyping

All of the studies performed were approved by the Institutional Animal Care and Use Committee (IACUC) of the University of Massachusetts Medical School. Animals were maintained in a 12 h light/dark cycle. $Hig2^{fl/fl}$ animals were derived and genotyped as previously described [24]. $Hig2^{fl/fl}$ animals were crossed to an Adiponectin cre+ mouse line (B6;FVB-Tg(Adipoq-cre)1Evdr/J, Jackson Laboratories). $Hig2^{fl/fl}$ animals were also crossed to a Ucp1 cre+ mouse line (B6.FVB-Tg(Ucp1-cre)1Evdr/J, Jackson Laboratories). Cre genotyping was performed according to the method of Jackson Laboratories.

2.1.2. Diet and housing

At 4–6 weeks of age, male C57Bl/6J, $Hig2^{fl/fl}$, $Hig2^{fl/fl}$ Adiponectin cre+, or $Hig2^{fl/fl}$ Ucp1 cre+ littermate animals were placed on a high fat diet (60% fat, D12492i or 45% fat, D12451 (Figure 1 only), Research Diets) or fed chow (Lab Diet 5P76) for 8,12,16 or 20 weeks. Animals were switched to thermoneutral housing (30 °C, 12 h light/dark cycle) for 4 weeks and retained on the same diet they were previously fed.

2.1.3. Insulin and glucose tolerance tests

Mice were fasted 16 h for glucose tolerance tests and 4 h for insulin tolerance tests. Mice were injected IP with 1 g/kg of glucose or 1 IU/kg of insulin, blood was drawn from the tail vein at the indicated times, and blood glucose levels were measured with a Breeze-2-glucose meter (Bayer). Mice were euthanized by CO_2 inhalation followed by bilateral thoracotomy.

2.1.4. Metabolic cage studies

The metabolic cage studies were performed at the National Mouse Metabolic Phenotyping Center (MMPC) at UMass. Mice were fed HFD for 16 weeks and the metabolic cages were used to measure food intake, RER, VO_2 consumption, VCO_2 production, energy expenditure, fat and lean mass, and physical activity over a 3-day period, and an average for each parameter was calculated (TSE Systems).

2.2. Ex vivo lipolysis

Mice were fasted for 16 h and euthanized by CO_2 inhalation followed by bilateral thoracotomy. Epididymal adipose tissue was removed and cut into 80–100 mg pieces, placed in 0.5 ml Krebs-Ringer-Hepes (KRH) Buffer pH 7.4, supplemented with 2.5% fatty acid-free BSA and 1 mM sodium pyruvate. Samples were incubated in a 37 °C shaking water bath with or without 10 μM isoproterenol (Sigma, I5627) for 2 h and glycerol release into KRH was measured using a calorimetric assay (Sigma) according to the manufacturer's instructions and normalized to the fat pad weight.

2.3. Adipose tissue fractionation

Whole fat pads were isolated, minced, and placed in 5 ml Hanks Balanced Salt Solution, pH 7.4, supplemented with 5% fatty acid-free BSA and 1 mg/ml collagenase. Samples were incubated in a 37 °C

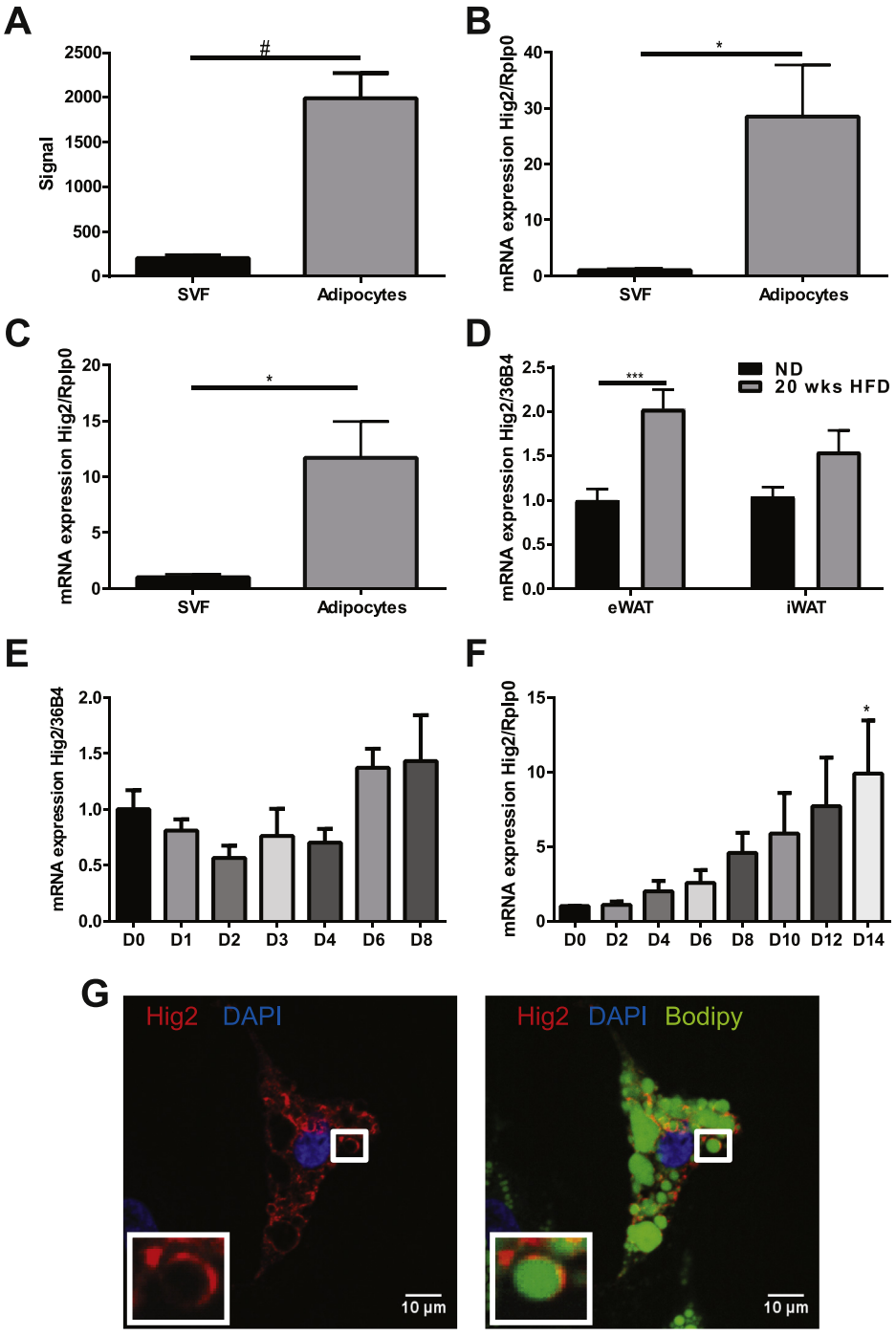

Figure 1: Hig2 localizes to lipid droplets in human cultured adipocytes and its expression increases with adipogenesis and obesity. A–C, Adipose tissue was isolated from patients undergoing bariatric surgery. A, microarray from omental adipose tissue. (#, $p < 0.0001$, $n = 6$). B, C qRT-PCR was performed on indicated tissues for Hig2 and normalized to Rplp0. B, fractionated omental adipose tissue. (*, $p < 0.05$, $n = 6–7$). C, fractionated subcutaneous adipose tissue. (*, $p < 0.05$, $n = 7–8$). Data are represented as the mean ± S.E. D, C57BL/6J animals were fed HFD for 20 weeks, eWAT and iWAT were isolated, RNA was extracted, and qRT-PCR was performed for Hig2 and normalized to 36B4. (***, $p < 0.005$, $n = 7–8$). Data are represented as the mean ± S.E. E, 3T3-L1 cells were differentiated, RNA was extracted on the indicated day, and qRT-PCR was performed for Hig2 and normalized to 36B4. ($n = 3–7$). Data are represented as the mean ± S.E. F, SGBS cells were differentiated, RNA was extracted on the indicated day, and qRT-PCR was performed for Hig2 and normalized to Rplp0. (*, $p < 0.05$, one-way analysis of variance, $n = 3–7$). Data are represented as the mean ± S.E. G, SGBS cells were fixed Day 10 post-differentiation. Cells were stained with Hig2 (*red*), Bodipy (*green*), and DAPI (*blue*). Left, merge of Hig2 and DAPI, right, merge of Hig2, Bodipy, and DAPI.

shaking water bath for 45 min, and the digestion reaction was terminated with 5 ml of HBSS and BSA. Tissue was filtered through a 200 µM filter, spun at 200× g for 5 min, and adipocyte and stromal vascular fractions (SVF) were separated. Both were washed with HBSS 2× and then placed in TriPure for RNA isolation.

2.4. Plasma and lipid analysis

Mice were fasted for 16 h for plasma lipid analysis. Blood was taken via cardiac puncture, and EDTA-containing plasma was collected. Total serum cholesterol levels (ab65359 Abcam), serum triglyceride levels (Triglyceride Determination Kit, Sigma), serum non-esterified fatty

acids (NEFAs) (Wako Diagnostics), and serum glycerol (Free Glycerol Determination Kit, Sigma) were measured using calorimetric assays according to the manufacturer's instructions. Insulin and adiponectin levels (Millipore) were measured by ELISA according to manufacturer's instructions.

2.5. Triglyceride and cholesterol extraction

Whole livers were isolated and flash frozen in liquid nitrogen. Lipids were extracted from livers via the Folch method [25]. Lipids were dissolved in isopropanol with 1% Triton-X100. Triglyceride (Triglyceride Determination Kit, Sigma) and cholesteryl ester (ab65359 Abcam) levels were measured using calorimetric assays according to the manufacturer's instructions and normalized to liver weight.

2.6. Human samples

Human adipose tissue samples were collected from morbidly obese patients who underwent gastric bypass surgery between 2005 and 2009 at the University of Massachusetts Medical School [26]. Samples used for microarray analysis were from BMI-matched female patients, whereas qRT-PCR validations were performed in samples from both males and females. Adipose tissue samples were obtained from lower abdominal wall (for subcutaneous) and omentum (for visceral) during the surgery. Informed consent was given by the patients and the study was approved by University of Massachusetts Medical School Institutional Review Board. Microarray data have been deposited in GEO database under accession code GSE20950.

2.7. RNA isolation and RT-qPCR

Total RNA was isolated from cells or tissues using TriPure isolation reagent (Roche) according to the manufacturer's protocol. The isolated RNA was DNase treated (DNA-free, Life Technologies), and cDNA was synthesized using iScript cDNA synthesis kit (BioRad). RT-qPCR was performed on the BioRad CFX96 using iQ SybrGreen supermix and 36B4 served as the reference gene. Primer sequences are as follows: 36B4 (5′-TCCAGGCTTTGGGCATCA-3′, 5′-CTTTATCAGCTGCACATCACTCAGA-3′); Hig2 (5′-CATGTTGACCCTGCTTTCCAT-3′, 5′-GCTCTCCAGTAAGCCTCCCA-3′); Human Primers: RPLP0 (5′-CAGATTGGCTACCCAACTGTT-3′, 5′-GGGAAGGTGTAATCCGTCTCC-3′); HIG2 (5′-AAGCATGTGTTGAACCTCTACC-3′, 5′-GATGGAGAGTAGGGTCAGTACC-3′).

2.8. Cell culture

3T3-L1 fibroblasts were grown and differentiated into adipocytes as previously described [27]. Simpson-Golabi-Behmel syndrome (SGBS) cells were obtained from Dr. Martin Wabitsch's laboratory. SGBS fibroblasts were grown and differentiated into adipocytes as previously described with modifications [28]. Briefly, SGBS fibroblasts were grown to confluence in DMEM/F12 containing 10% fetal bovine serum, 33 μM biotin, 17 μM pantothenic acid, 50units/ml penicillin, and 50 μg/ml streptomycin. Two days after confluence, serum-free differentiation medium (25 nM dexamethasone, 250 μM 1-methyl-3-isobutylxanthine, 0.01 mg/ml transferrin, 0.2 nM triiodothyronine, 20 nM human insulin, 2 μM rosiglitazone, and 100 nM cortisol) was added. Four days later, the differentiation cocktail was replaced with maintenance medium (DMEM/F12, biotin, pantothenic acid, transferrin, insulin and cortisol). Cells were considered fully mature 14 days post-differentiation.

2.9. Cell imaging

Cells were fixed in 10% buffered formalin in PBS for 1 h, blocked in 1% normal goat serum in PBS for 1 h at room temperature, incubated with Hig2 antibodies (1:100, Rockland Immunochemicals [24]) for 2 h at room temperature, incubated with fluorescent secondary antibodies 1:1000 for 1 h, treated with Bodipy 493/503 (ThermoFisher, D-3922) at 1:10,000 for 15 min, and mounted with Prolong Gold with DAPI (Life Technologies). Cells were imaged at room temperature with a Solamere Technology Group modified Yokogawa CSU10 Spinning Disk Confocal with a Nikon TE-2000E2 inverted microscope at 60×.

2.10. Histology

Tissues were isolated and fixed in 10% formalin, embedded in paraffin, sectioned, and stained with hematoxylin and eosin (H&E). The UMass Morphology Core performed the embedding, sectioning, and staining.

2.11. Statistical analysis

Data were analyzed in GraphPad Prism 6 (GraphPad Software, Inc.). A two-tailed student's t test with Welch's Correction was used to compare two groups of data. Where indicated, data were analyzed using a one-way ANOVA or a two-way ANOVA with repeated measures. $P < 0.05$ was considered to be significant. The Grubb's test was used to determine if there were statistical outliers and if an outlier was determined, it was removed from the statistical analysis. Variance was estimated using standard error of the mean.

3. RESULTS

3.1. Hig2 localizes to lipid droplets in human cultured adipocytes and its expression increases with adipogenesis and obesity

As part of an effort to identify genes associated with obesity and insulin resistance, we performed microarray gene expression analyses on omental adipose tissue from human patients undergoing bariatric surgery after fractionation into adipocytes and stromal vascular fraction (SVF) [26] and sorted genes by adipocyte specificity. One of the top gene hits that displayed 10-fold enrichment in signal in the adipocyte fraction compared with SVF was Hig2 (Figure 1A). To validate this result, we performed qRT-PCR and Hig2 expression was 28-fold higher in human omental adipocytes (Figure 1B) and 12-fold higher in human subcutaneous adipocytes (Figure 1C) compared with the respective SVFs. We demonstrated previously that Hig2 expression increased with lipid deposition in mouse liver [24]. To investigate whether this was also the case in adipose tissue, we placed wild type mice on a HFD for 20 weeks, and measured Hig2 expression in epididymal white adipose tissue (eWAT) and inguinal WAT (iWAT) by qRT-PCR. Although it was unchanged in iWAT, Hig2 expression in eWAT of wild type animals doubled with high-fat-feeding (Figure 1D).

As LD proteins often display increases in expression with adipogenic differentiation [29–33], we also measured Hig2 expression by qRT-PCR in an adipocyte cell line and an adipocyte cell strain upon adipogenic stimulation. In the murine 3T3-L1 adipocyte cell line, Hig2 expression was unchanged with differentiation (Figure 1E); however, its expression was increased by 10-fold after 14 days of adipogenic differentiation in the human Simpson-Golabi-Behmel syndrome (SGBS) adipocyte cell strain (Figure 1F). We verified this result by assessing endogenous Hig2 protein expression in SGBS cells on day 10, post-differentiation by immunofluorescence. Interestingly, Hig2 (red) localized to Bodipy-positive (green) LDs, as previously observed in primary hepatocytes [24], demonstrating that Hig2 is also a LD protein in human adipocytes (Figure 1G).

3.2. Adipocyte-specific Hig2 deficient animals display improved glucose homeostasis when BAT is active

To further investigate the role of adipocyte-specific Hig2, mice with adipocyte-specific Hig2 deficiency (Hig2AdKO) were generated by

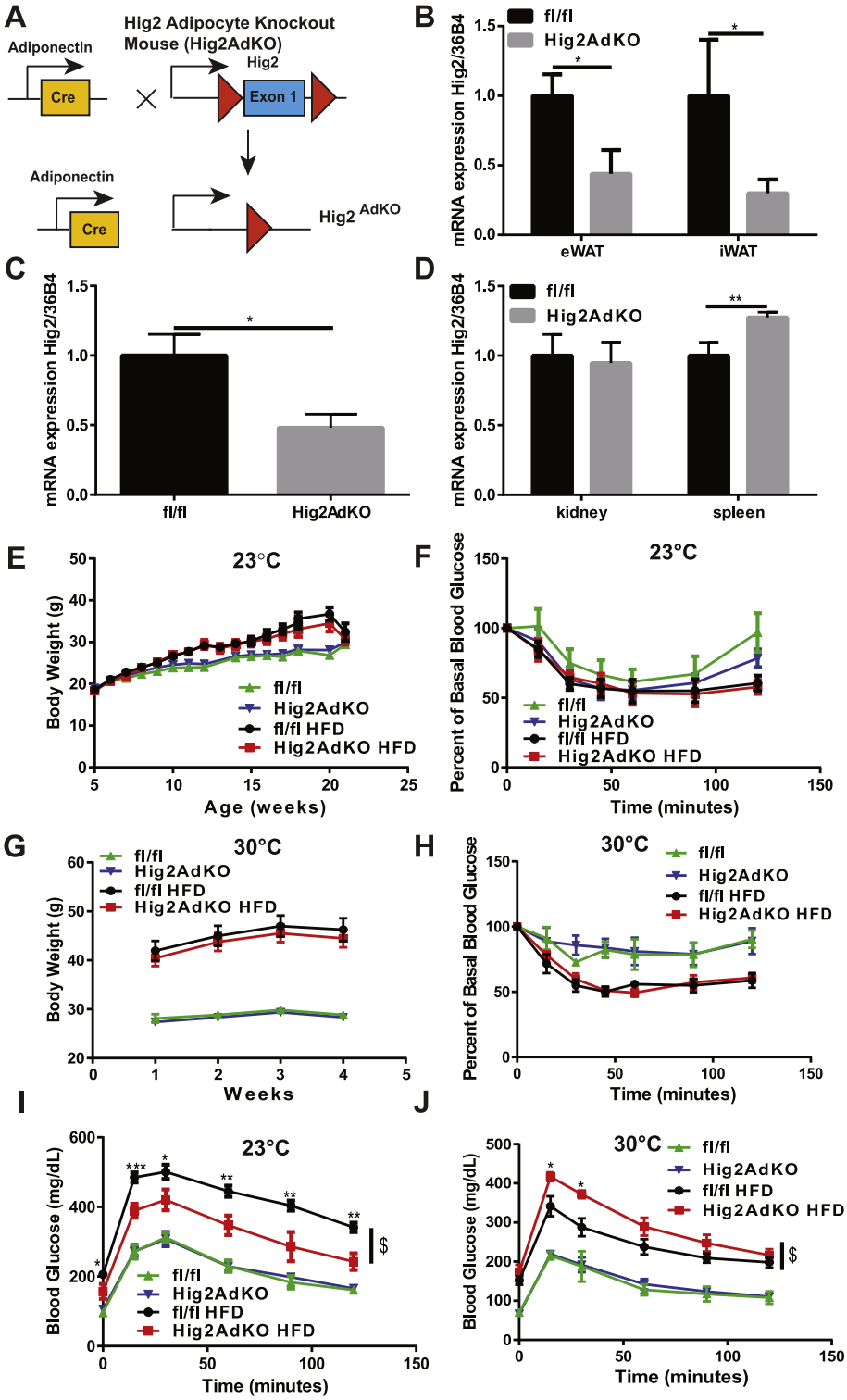

Figure 2: Adipocyte-specific Hig2 deficient animals display improved glucose homeostasis when BAT is active. A, schematic of adiponectin-cre-mediated Hig2 deletion. B–D, indicated tissues were isolated from fl/fl and Hig2AdKO mice, RNA was extracted, and qRT-PCR was performed for Hig2 and normalized to 36B4. B, isolated epididymal and inguinal adipocytes. (*, $p = 0.05$, $n = 3–9$). C, brown adipose tissue. (*, $p < 0.05$, $n = 5–8$). D, kidney and spleen. (**, $p < 0.01$, $n = 4–10$). Data are represented as the mean ± S.E. E,F,I, fl/fl or Hig2AdKO animals were fed ND or HFD at 23 °C for 16 weeks. G,H,J, fl/fl or Hig2AdKO animals were fed ND or HFD for 8 weeks, then moved to 30 °C for 4 weeks. E, body weight curves at 23 °C. ($n = 8–20$). F, insulin tolerance test at 23 °C. ($n = 4–13$). G, body weight curves at 30 °C. ($n = 3–9$). H, insulin tolerance test at 30 °C. ($n = 3–5$). I, glucose tolerance test at 23 °C. (*, $p < 0.05$, **, $p < 0.01$, ***, $p < 0.001$, $, $p < 0.005$, two-way analysis of variance, $n = 5–13$). J, glucose tolerance test at 30 °C. (*, $p < 0.05$, $, $p < 0.05$, two-way analysis of variance, $n = 3–10$). Data are represented as the mean ± S.E.

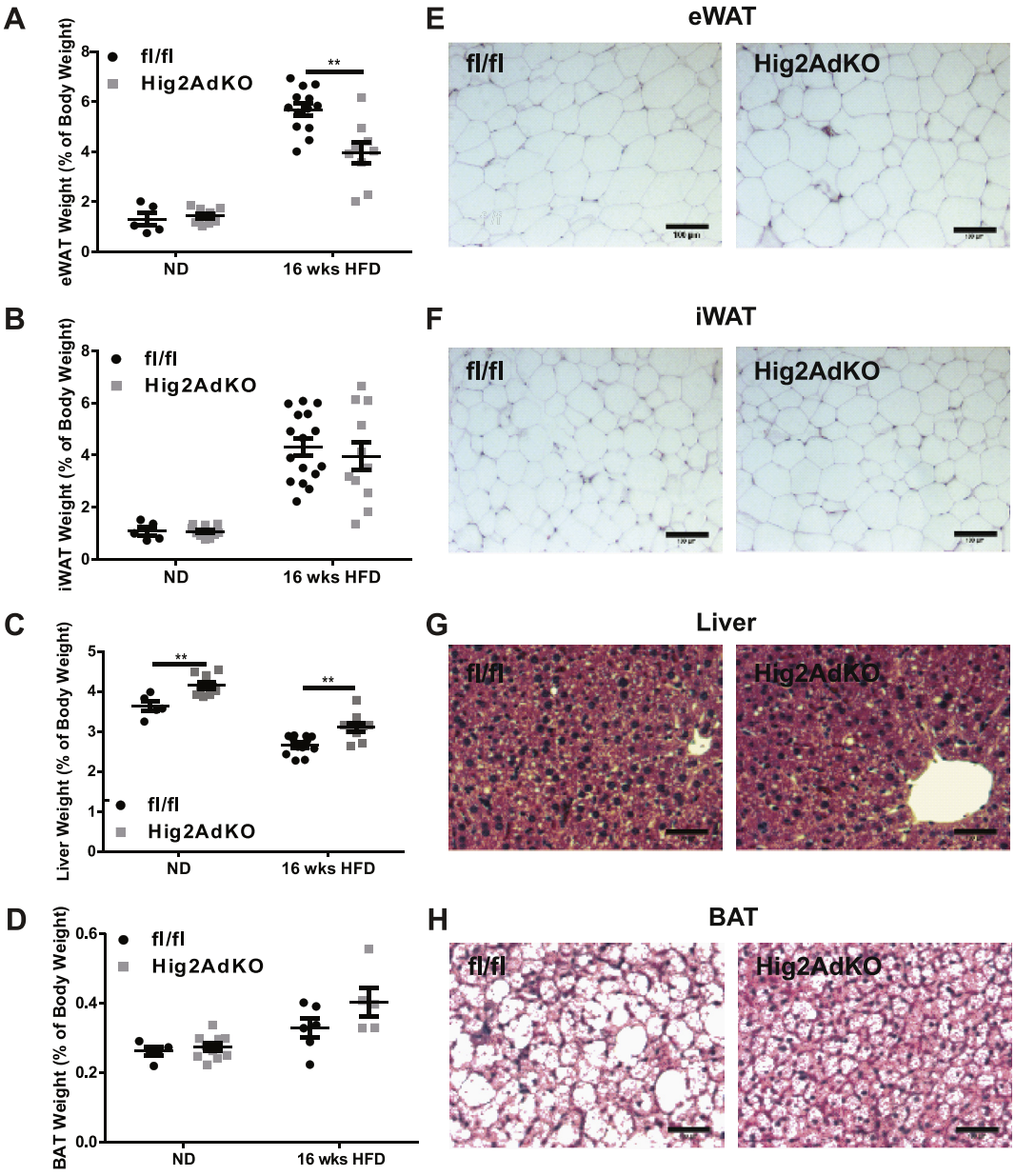

Figure 3: Adipocyte-specific Hig2 deficiency alters adipose tissue distribution in HFD-fed mice at 23 °C. A–H, fl/fl or Hig2AdKO animals were fed ND or HFD for 16 weeks. A–D, Tissues were weighed and normalized to body weight. A, eWAT. (**, $p < 0.01$, $n = 5–13$). B, iWAT. ($n = 5–14$). C, liver. ($n = 5–10$). D, BAT. (**, $p < 0.01$, $n = 5–12$). Data are represented as individual values ± S.E. E–H, HFD tissues were sectioned and stained with H&E. E, eWAT. F, iWAT. G, liver. H, BAT.

crossing Hig2$^{fl/fl}$ mice with Adiponectin cre+ mice (Figure 2A). To determine whether the deletion was adipocyte-specific, we isolated adipocytes from eWAT and iWAT and performed qRT-PCR for Hig2. As expected, there was a significant 60% reduction in Hig2 mRNA expression in eWAT and 70% reduction in iWAT in Hig2AdKO animals compared with fl/fl littermate controls (Figure 2B). There was also a significant 50% reduction in Hig2 expression in whole BAT but no change in non-adipose tissues such as kidney and spleen, demonstrating that the deletion is specific to adipocytes (Figure 2C,D).

Mice are typically housed at 23 °C, which presents a cold stress and persistent activation of thermogenic pathways. Cold stress increases catecholamine levels, thereby activating nonshivering thermogenesis in BAT and substantially increasing food intake and metabolic rate [22]. Thus, it has been informative to characterize mouse models with genetic alterations in energy storage at room temperature (23 °C) versus thermoneutrality (30 °C), a temperature that poses no thermal stress and little BAT activation [23,34,35]. Recently, it has been demonstrated that housing mice with LD protein deficiencies at thermoneutrality reveals phenotypes that more closely resemble lipodystrophic syndromes in humans with mutations in LD protein genes [36]. For these reasons, Hig2AdKO animals were fed chow or HFD for 16 weeks at 23 °C and maintained at the same temperature, or fed chow or HFD for 16 weeks at 23 °C then moved to 30 °C for four weeks, and metabolic parameters were assessed.

There were no significant differences in body weight (fat or lean mass), or insulin sensitivity as measured by an insulin tolerance test (ITT),

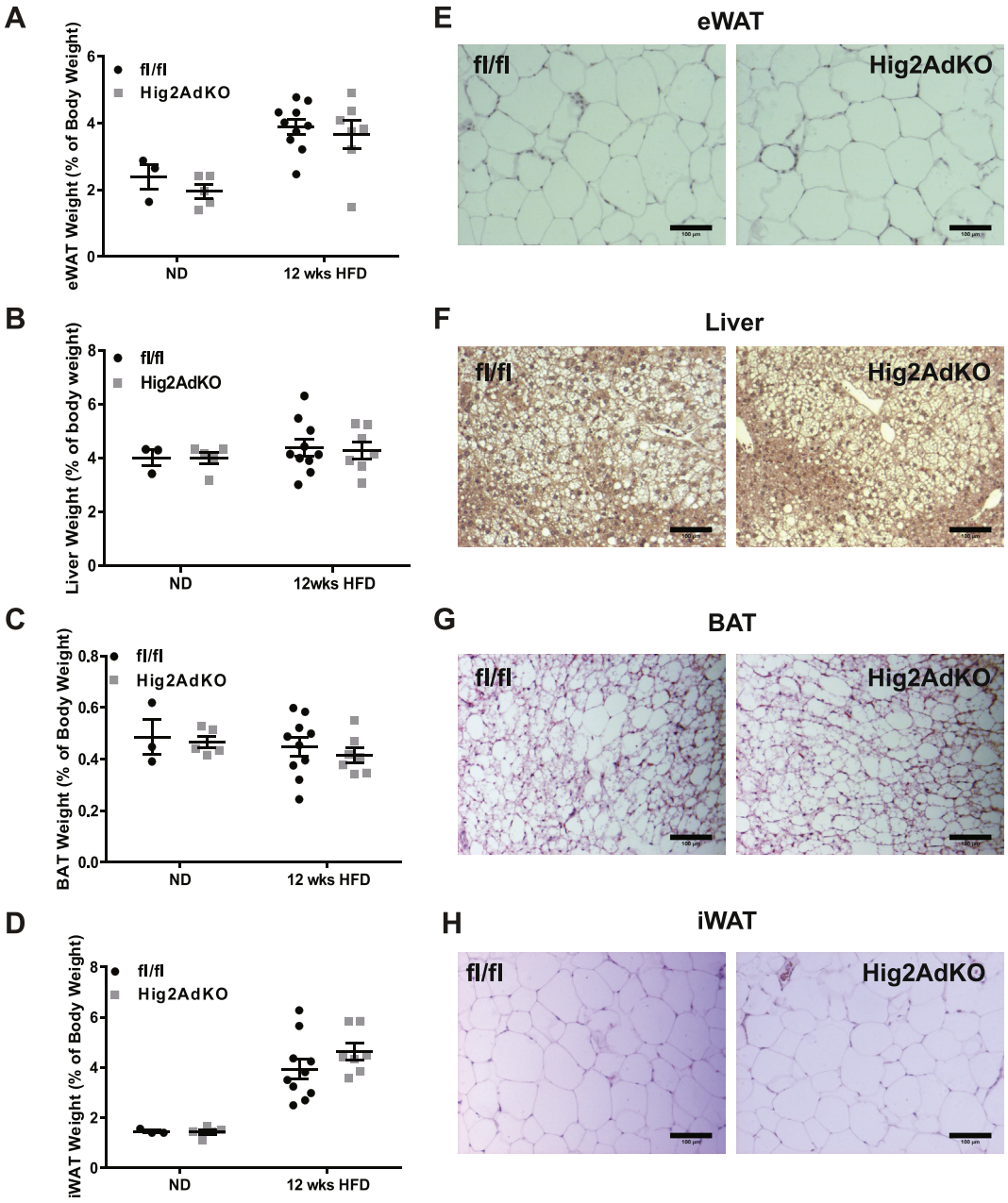

Figure 4: Thermoneutrality abrogates the altered fat distribution in Adipocyte-specific Hig2-deficient mice. A–H, fl/fl or Hig2AdKO animals were fed ND or HFD for 8 weeks, then moved to 30 °C for 4 weeks. A–D, Tissues were weighed and normalized to body weight. A, eWAT. (n = 3–10). B, liver. (n = 3–10). C, BAT. (n = 3–10). D, iWAT. (n = 3–10). Data are represented as individual values ± S.E. E–H, the indicated tissues were sectioned and stained with H&E. E, eWAT. F, liver. G, BAT. H, iWAT.

energy expenditure, or respiratory exchange rate (RER) between genotypes in either feeding condition at 23 °C (Figure 2E,F, Supplementary Figure 1) or 30 °C (Figure 2G,H), but Hig2AdKO animals had significantly improved glucose tolerance compared with fl/fl littermates in the high-fat-fed condition as measured by a glucose tolerance test (GTT) at 23 °C (Figure 2I), suggesting that adipocyte Hig2 promotes glucose intolerance in diet-induced obesity. Although insulin levels are significantly increased in Hig2AdKO animals after 16 weeks high-fat feeding (Supplementary Table 1), they are likely not the cause of the improved glucose tolerance in these animals, as glucose tolerance is also improved in Hig2AdKO animals fed HFD for 8 weeks, a time point when insulin levels are unchanged (Supplementary Figure 2). In contrast, HFD-fed Hig2AdKO animals surprisingly had a significantly worsened glucose intolerance compared with fl/fl controls after four weeks of housing at thermoneutral temperature (Figure 2J). This represented a marked reversal in the metabolic consequences of Hig2 deficiency that was dependent on housing temperature, which is similar to the phenotype of Fsp27-deficient animals [36].

3.3. Adipocyte-specific Hig2 deficiency alters adipose tissue distribution in HFD-fed mice at 23 °C

LD protein deficiencies alter lipid deposition *in vivo* [10,11,37–40]. Thus, we examined fat pad and liver weights of fl/fl and Hig2AdKO animals at 23 °C. In chow-fed mice, eWAT and iWAT fat pad weights were unchanged between genotypes (Figure 3A,B). However, upon HFD-feeding, Hig2AdKO animals had significantly reduced eWAT

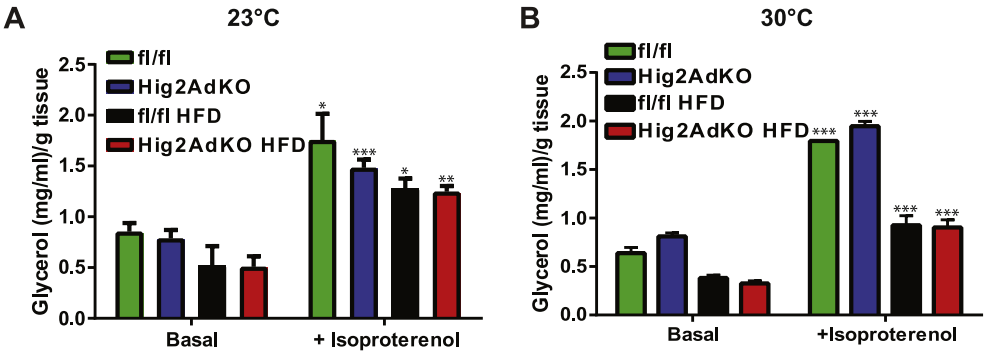

Figure 5: Adipocyte-specific Hig2 deficiency does not alter *ex vivo* glycerol release. A, fl/fl or Hig2AdKO animals were fed ND or HFD for 16 weeks at 23 °C. A, *ex vivo* lipolysis of eWAT. (*, $p < 0.05$, **, $p < 0.01$, ***$p < 0.005$, $n = 3–5$). Data are represented as the mean ± S.E. B, fl/fl or Hig2AdKO animals were fed ND or HFD for 8 weeks at 23 °C and then moved to 30 °C for 4 weeks. B, *ex vivo* lipolysis of eWAT. (***, $p < 0.005$, $n = 3–10$). Data are represented as the mean ± S.E.

weight compared with fl/fl controls (3.9 ± 0.4% vs 5.7 ± 0.2%), while iWAT weight was unchanged (Figure 3A,B). This reduction corresponded to a concomitant increase in liver weight from 2.7 ± 0.07% of body weight in controls to 3.1 ± 0.11% in Hig2AdKO animals (Figure 3C). Chow-fed Hig2AdKO animals also had significantly increased liver weight compared with fl/fl littermates (Figure 3C).

The reduction in eWAT weight suggests that Hig2 deficiency reduces depot-specific fat deposition. Thus, H&E-stained histology from HFD animals was examined to determine whether there were visible alterations in AT and liver to complement the weight differences. While eWAT, iWAT, and liver histology appeared unchanged between the genotypes (Figure 3E,F,G), there was a striking visible reduction in lipids in BAT of Hig2AdKO animals compared with fl/fl controls (Figure 3H). There were no differences in BAT weight between genotypes in the ND or HFD-fed mice (Figure 3D). Taken together, these results suggest that adipocyte-specific Hig2 deficiency alters adipose tissue distribution in obesity.

3.4. Thermoneutrality abrogates the altered fat distribution in adipocyte-specific Hig2-deficient mice

As glucose intolerance on HFD was worsened with thermoneutral housing, we also assessed alterations in fat distribution in the Hig2AdKO animals at 30 °C. Indeed, the reduction in eWAT weight that was observed in Hig2AdKO animals at 23 °C was abrogated when the animals were placed at thermoneutrality (Figure 4A). Furthermore, the increase in liver weight that was observed in Hig2AdKO animals at 23 °C was also suppressed (Figure 4B); however, there continued to be no difference in iWAT or BAT weight between genotypes (Figure 4C,D). Additionally, H&E-stained histology sections of eWAT, iWAT, BAT, and liver were examined and no visual differences were observed between fl/fl and Hig2AdKO animals (Figure 4E—H). This was in striking contrast from 23 °C, at which temperature the Hig2AdKO mouse BAT was cleared of lipids (Figure 3H). Thus, all phenotypic differences in fl/fl vs. Hig2AdKO mice were abrogated at thermoneutrality (glucose tolerance, eWAT weight, liver weight, BAT lipid content), which suggests that these parameters may be mediated by BAT function that is dependent on activation of BAT by cold stress.

3.5. Adipocyte-specific Hig2 deficiency does not alter ex vivo glycerol release

We have previously demonstrated that Hig2 deficiency increased lipolysis in hepatocytes [24], and thus investigated the role of Hig2 deficiency in controlling these parameters in adipocytes. We measured *ex vivo* glycerol release from eWAT explants of fl/fl and Hig2AdKO animals in basal and isoproterenol-stimulated conditions, and found no difference between genotypes at 23 °C (Figure 5A) or 30 °C (Figure 5B). Serum non-esterified fatty acids (NEFAs) and serum glycerol, two systemic measures of lipolysis, were also found to be unchanged between genotypes at 23 °C (Supplementary Table 1) and 30 °C (Supplementary Table 2).

3.6. Brown adipocyte-specific Hig2 deficiency is sufficient to improve glucose tolerance at 23 °C

Thermoneutrality abrogated the improvement in glucose tolerance mediated by adipocyte-specific Hig2 deficiency and thermoneutrality reduces both lipolysis and brown fat activity [41]. We crossed $Hig2^{fl/fl}$ animals with brown and beige/brite adipocyte-specific Ucp1 cre+ animals to generate brown adipocyte-specific Hig2 knockout animals (Hig2BATKO) and elucidate the role of Hig2 specifically in the brown adipocyte (Figure 6A). Tissues from fl/fl and Hig2BATKO animals were excised to assess deletion specificity. There was a significant reduction in Hig2 mRNA in whole BAT as measured by qRT-PCR (Figure 6B), but no reduction in other tissues including white adipocytes, spleen, or kidney (Figure 6C,D), demonstrating that the deletion is specific. Interestingly, Hig2 expression was upregulated by approximately 7-fold in eWAT adipocytes of Hig2BATKO animals compared with floxed controls (Figure 6C).

To evaluate the role of brown adipocyte-specific Hig2 deficiency on whole body metabolism, fl/fl and Hig2BATKO animals were placed on chow or HFD for 8 weeks at 23 °C or placed on HFD for 4 weeks at 23 °C and moved to 30 °C for four weeks and metabolic parameters were assessed. There were no differences in body weight or insulin sensitivity between the genotypes at 23 °C (Figure 6E,F) or 30 °C (Figure 6G,H). However, when challenged with a GTT, HFD-fed Hig2BATKO animals at 23 °C were significantly more glucose tolerant compared to their fl/fl control littermates (Figure 6I), similar to the Hig2AdKO animals (Figure 2I). Furthermore, this improvement in glucose tolerance in the Hig2BATKO animals was abrogated by thermoneutral housing (Figure 6J), similar to the Hig2AdKO animals (Figure 2J). The loss of improved glucose tolerance at thermoneutrality in both animal models suggests that Hig2 deletion in active brown fat mediates the observed improvements in glucose tolerance.

3.7. Brown adipocyte-specific Hig2 deficiency does not alter adipose tissue distribution at 23 °C

To determine whether Hig2 deficiency in brown adipocytes was responsible for the reduced eWAT weight and increased liver weight in

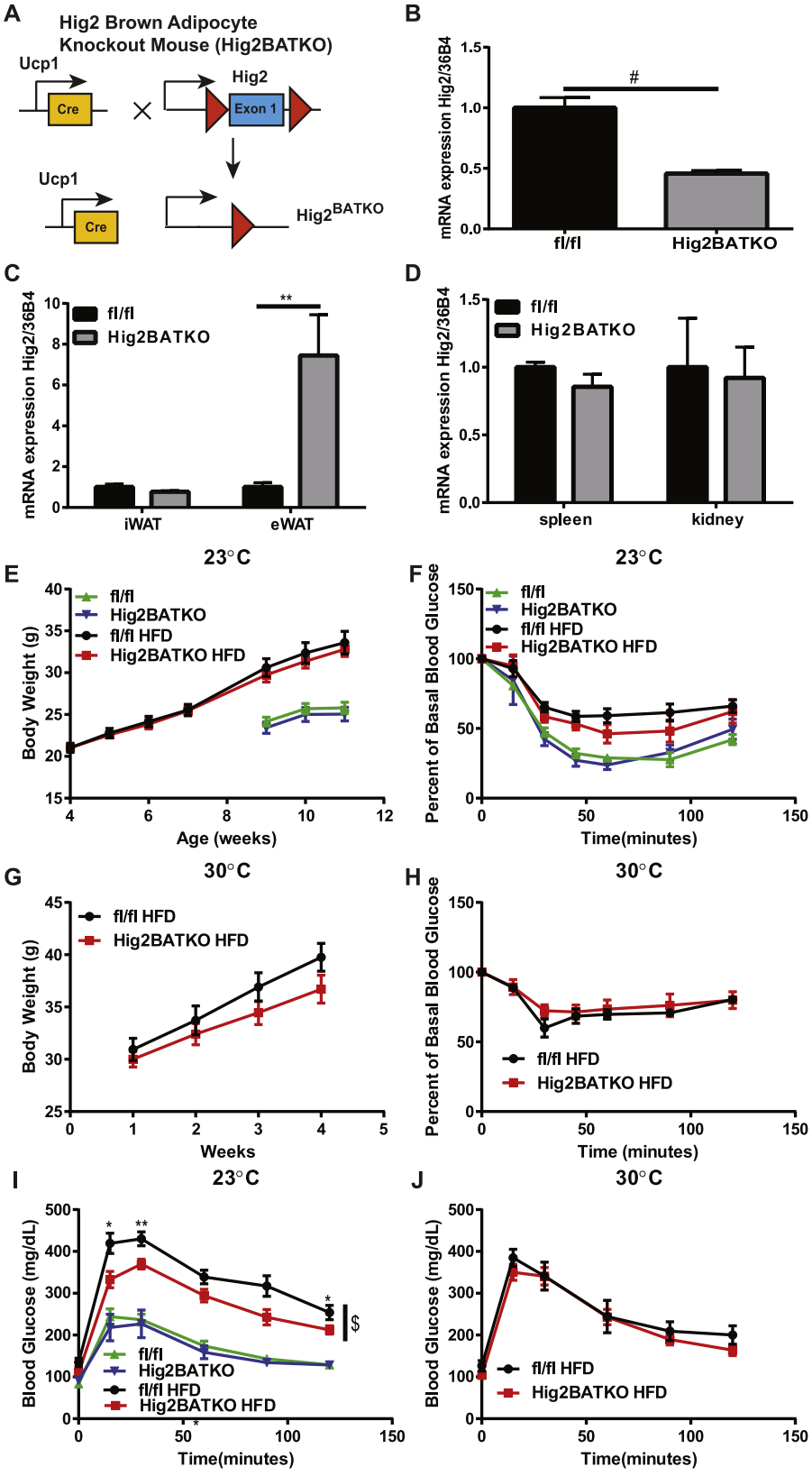

Figure 6: Brown adipocyte-specific Hig2 deficiency is sufficient to improve glucose tolerance at 23 °C. A, schematic of Ucp1-cre-mediated Hig2 deletion. B–D, indicated tissues were isolated from fl/fl and Hig2BATKO mice, RNA was extracted, and qRT-PCR was performed for Hig2 and normalized to 36B4. B, brown adipose tissue. (#, $p < 0.001$, $n = 7$). C, isolated inguinal (iWAT) and epididymal (eWAT) adipocytes. (**, $p < 0.01$, $n = 3–7$). D, kidney and spleen. ($n = 3–8$). Data are represented as the mean ± S.E. E,F,I, fl/fl or Hig2BATKO animals were fed ND or HFD at 23 °C for 8 weeks. G,H,J, fl/fl or Hig2BATKO animals were fed ND or HFD for 4 weeks, then moved to 30 °C for 4 weeks. E, body weight curves at 23 °C. ($n = 5–10$). F, insulin tolerance test at 23 °C. ($n = 3–10$). G, body weight curves at 30 °C. ($n = 8$). H, insulin tolerance test at 30 °C. ($n = 3–8$). I, glucose tolerance test at 23 °C. (*, $p < 0.05$, **, $p < .01$, $, $p < 0.05$, two-way analysis of variance, $n = 5–13$). J, glucose tolerance test at 30 °C. ($n = 5–11$). Data are represented as the mean ± S.E.

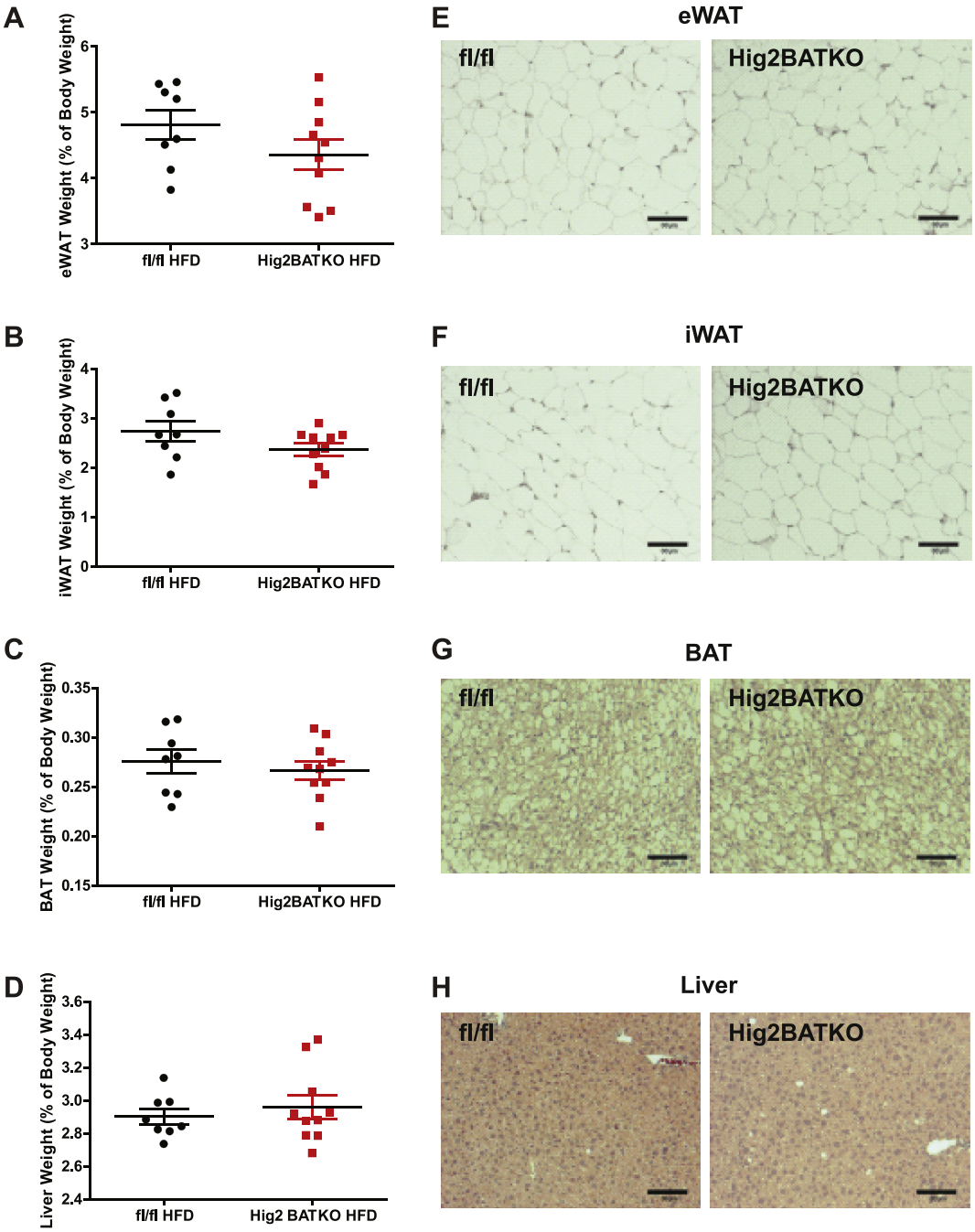

Figure 7: Brown adipocyte-specific Hig2 deficiency does not alter adipose tissue distribution at 23 °C. A—H, fl/fl or Hig2BATKO animals were fed HFD for 8 weeks. A—D, Tissues were weighed and normalized to body weight. A, eWAT. (n = 8—10). B, iWAT. (n = 8—10). C, BAT. (n = 8—10). D, liver. (n = 8—10). Data are represented as individual values ± S.E. E—H, the indicated tissues were sectioned and stained with H&E. E, eWAT. F, iWAT. G, BAT. H, Liver.

Hig2AdKO animals, liver and fat pads from fl/fl and Hig2BATKO animals after 8 weeks of HFD at 23 °C were weighed. It was observed that eWAT, iWAT, BAT and liver weights were unchanged between genotypes (Figure 7A—D), in contrast to the phenotype observed in the animals lacking Hig2 in all adipose depots. In accordance with these results, H&E-stained histological sections of eWAT, iWAT, BAT, and liver appeared to be unchanged between Hig2BATKO animals and fl/fl controls (Figure 7E—H). Taken together, these results demonstrate that brown adipocyte-specific Hig2 deficiency alone is not sufficient to redistribute fat deposition in WAT as observed in the Hig2AdKO animals.

3.8. Brown adipocyte-specific Hig2 deficiency does not alter ex vivo glycerol release

We also measured glycerol release into media of eWAT explants from Hig2BATKO and fl/fl controls and did not observe any differences between genotypes in mice housed at 23 °C (Figure 8A) or at thermoneutrality (Figure 8B), similar to the results observed from adipocyte-specific Hig2 deficient mice suggesting that both brown and white adipose tissue Hig2 is not required for inhibition of adipose tissue lipolysis and glycerol release. Additionally, serum NEFAs and glycerol, both measures of lipolysis, were also unchanged at 23 °C

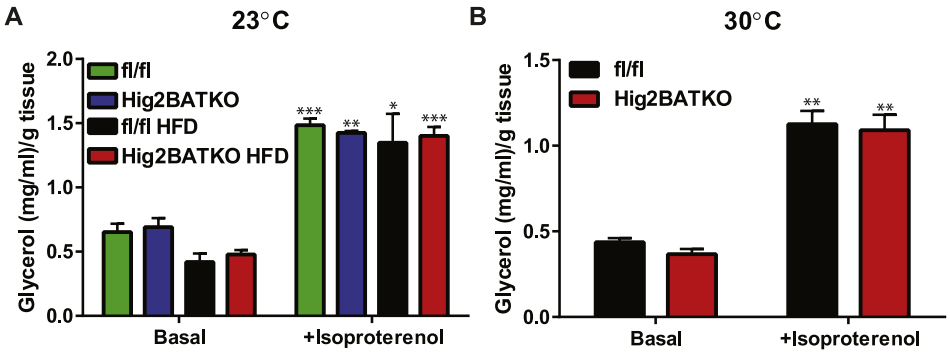

Figure 8: Brown adipocyte-specific Hig2 deficiency does not alter *ex vivo* glycerol release. A, fl/fl or Hig2BATKO animals were fed HFD for 8 weeks at 23 °C. A, *ex vivo* lipolysis of eWAT. (*, $p < 0.05$, **, $p < 0.01$, ***, $p < 0.005$ $n = 3–8$). Data are represented as the mean ± S.E. B, fl/fl or Hig2BATKO animals were fed HFD for 4 weeks at 23 °C and then moved to 30 °C for 4 weeks. B, *ex vivo* lipolysis of eWAT (**, $p < 0.01$ $n = 3–6$). Data are represented at the mean ± S.E.

(Supplementary Table 3) and 30 °C (Supplementary Table 4). Taken together, these data suggest that Hig2 localizes to LDs in human adipocytes without regulating lipolytic processes, but instead has a surprising function to promote glucose intolerance in mice.

4. DISCUSSION

Adipose tissue is a critical metabolic organ and BAT and WAT display distinct metabolic functions. While WAT functions in energy storage, active BAT promotes energy consumption. Their functions and physiology suggest that LDs and LD proteins may differ between tissues. As such, recent studies have suggested that LD proteins such as Fsp27 can have tissue-specific roles, and that their physiological functions vary depending on environmental conditions, which can alter BAT activity [36]. In this study, we demonstrate that Hig2 also has tissue-specific roles and has varying physiological function in different environmental conditions.

Hig2 deficiency in adipocytes (Figure 2) reduced eWAT mass, largely cleared BAT of lipids, and improved HFD-mediated glucose intolerance *in vivo* (Figures 2I and 3A,H). Interestingly, these improvements were abrogated when the animals were placed at thermoneutrality for 4 weeks (Figures 2J and 4A,G), suggesting that BAT activity or other physiological responses to cold stress mediated these effects. To test that hypothesis, *ex vivo* glycerol release was measured in eWAT from animals housed at room temperature and thermoneutrality and was unchanged between the genotypes (Figure 5A,B). Serum NEFAs and serum glycerol, two systemic measures of lipolysis, were also unchanged (Supplementary Tables 1 and 2). These data suggest that Hig2 could be promoting lipid deposition in adipocytes by a different mechanism than lipolytic inhibition, although the exact mechanism is currently unclear. Recent data suggest that lipolytic regulation in adipose tissue and liver may differ. Cgi-58 physically interacts with Atgl and promotes lipolysis in adipocytes [42]. However, it has recently been demonstrated that Cgi-58 regulates hepatic lipid storage both in the presence and in the absence of Atgl, suggesting that their physical interaction may not be necessary to promote lipolysis in hepatocytes [43]. Additionally, Perilipin 1 is present in adipocytes, but absent in hepatocytes, where Perilipins 2/3 are tissue-specific PAT proteins and Perilipins 2/3 do not inhibit lipolysis as efficiently as Perilipin 1 [6,11]. Further work will need to be done to pinpoint the tissue-specific differences in lipolytic signaling.

To examine the role of brown-adipocyte-specific Hig2, Hig2BATKO animals were generated and metabolically characterized. These animals displayed no improvements in serum parameters, histology, or adipose tissue distribution, but had significantly improved glucose tolerance which was abrogated by thermoneutral housing, suggesting that brown adipocytes alone have little role to regulate the altered lipid deposition in eWAT or clearing of BAT lipids in Hig2AdKO animals, but play a significant role in the metabolic improvements that were observed (Supplementary Tables 3 and 4, Figures 6, 7). The mechanism whereby brown adipocyte-specific Hig2-deficiency prevents obesity-mediated glucose intolerance is currently unclear. *Ex vivo* glycerol release, serum NEFAs, and serum glycerol were unchanged between genotypes, suggesting that brown adipocyte-specific Hig2 deficiency does not alter lipolysis (Figure 8, Supplementary Tables 3 and 4) Unchanged food intake, oxygen consumption, energy expenditure, and RER in the Hig2AdKO animals (Supplementary Figure 1) suggest that improvements may be mediated independent of BAT thermogenesis. One possibility points to the putative endocrine function of BAT. Recent experiments suggest that, in addition to its thermogenic properties, activated BAT may function as an endocrine organ and can secrete beneficial molecules that improve overall metabolic health [44–48]. For instance, transplanting BAT into WAT of diabetic mice promoted adipogenesis and restored euglycemia [49]. Conflicting data suggest that although Hig2 may have an N-terminal signal sequence [50], it may be not be secreted [51], thus, future work is needed to investigate Hig2 as a putative factor secreted factor.

Metabolic characterization of the Hig2BATKO animals suggests that brown adipocyte-specific deficiency of Hig2 is not sufficient to alter fat distribution of WAT, but improves HFD-mediated glucose intolerance (Figures 6, 7). Future experiments targeting Hig2 specifically in white adipocytes would be useful to determine its true contribution to the phenotype of Hig2AdKO animals. Thermoneutrality experiments, which more accurately represent human living conditions, demonstrate that adipocyte-specific Hig2 deletion is detrimental to metabolic health (Figures 2 and 4). As Hig2 is localized to LDs in human adipocytes and is highly expressed in adipocytes of human subjects (Figure 1), it will be interesting to investigate whether there are rare human mutations in Hig2, much like the canonical LD proteins Perilipin 1, and Fsp27/Cidec [15,16,52], and if these mutations cause partial lipodystrophy and metabolic dysregulation. Future experiments to challenge the Hig2AdKO animals with cold exposure to evaluate glucose tolerance would be insightful due to hyper-activation of lipolysis and BAT at these temperatures [41]. Here, we have demonstrated that Hig2 expression promotes lipid deposition and diet-induced glucose intolerance in adipose tissue and liver [24]. Thus, it will be of interest to investigate the role of Hig2 in other tissues. LDs are relevant in a large variety of cells; thus, the role of Hig2 in lipid deposition in other tissues is still largely unanswered and is an active area of investigation.

ACKNOWLEDGEMENTS

We thank members of the Czech lab for helpful discussions. The MMPC at UMass is supported by the National Institutes of Health Grant: 2UC2-DK09300 to JKK.

CONFLICT OF INTEREST

We wish to confirm that there are no known conflicts of interest associated with this publication and there has been no significant financial support for this work that could have influenced its outcome.

APPENDIX A. SUPPLEMENTARY DATA

Supplementary data related to this article can be found at http://dx.doi.org/10.1016/j.molmet.2016.09.009.

REFERENCES

[1] Guilherme, A., Virbasius, J.V., Puri, V., Czech, M.P., 2008. Adipocyte dysfunctions linking obesity to insulin resistance and type 2 diabetes. Nature Reviews Molecular Cell Biology 9:367–377.

[2] Konige, M., Wang, H., Sztalryd, C., 2014. Role of adipose specific lipid droplet proteins in maintaining whole body energy homeostasis. Biochimica et Biophysica Acta 1842:393–401.

[3] Sethi, J.K., Vidal-Puig, A.J., 2007. Thematic review series: adipocyte biology. Adipose tissue function and plasticity orchestrate nutritional adaptation. Journal of Lipid Research 48:1253–1262.

[4] Zechner, R., Zimmermann, R., Eichmann, T.O., Kohlwein, S.D., Haemmerle, G., Lass, A., et al., 2012. Fat signals - lipases and lipolysis in lipid metabolism and signaling. Cell Metabolism 15:279–291.

[5] Robbins, A.L., Savage, D.B., 2015. The genetics of lipid storage and human lipodystrophies. Trends in Molecular Medicine 21:433–438.

[6] Brasaemle, D.L., 2007. Thematic review series: adipocyte biology. The perilipin family of structural lipid droplet proteins: stabilization of lipid droplets and control of lipolysis. Journal of Lipid Research 48:2547–2559.

[7] Xu, L., Zhou, L., Li, P., 2012. CIDE proteins and lipid metabolism. Arteriosclerosis, Thrombosis, and Vascular Biology 32:1094–1098.

[8] Greenberg, A.S., Coleman, R.A., Kraemer, F.B., McManaman, J.L., Obin, M.S., Puri, V., et al., 2011. The role of lipid droplets in metabolic disease in rodents and humans. Journal of Clinical Investigation 121:2102–2110.

[9] Gong, J., Sun, Z., Li, P., 2009. CIDE proteins and metabolic disorders. Current Opinion in Lipidology 20:121–126.

[10] Nishino, N., Tamori, Y., Tateya, S., Kawaguchi, T., Shibakusa, T., Mizunoya, W., et al., 2008. FSP27 contributes to efficient energy storage in murine white adipocytes by promoting the formation of unilocular lipid droplets. Journal of Clinical Investigation 118:2808–2821.

[11] Tansey, J.T., Sztalryd, C., Gruia-Gray, J., Roush, D.L., Zee, J.V., Gavrilova, O., et al., 2001. Perilipin ablation results in a lean mouse with aberrant adipocyte lipolysis, enhanced leptin production, and resistance to diet-induced obesity. Proceedings of the National Academy of Sciences of the United States of America 98:6494–6499.

[12] Brasaemle, D.L., Rubin, B., Harten, I.A., Gruia-Gray, J., Kimmel, A.R., Londos, C., 2000. Perilipin A increases triacylglycerol storage by decreasing the rate of triacylglycerol hydrolysis. Journal of Biological Chemistry 275:38486–38493.

[13] Greenberg, A.S., Egan, J.J., Wek, S.A., Garty, N.B., Blanchette-Mackie, E.J., Londos, C., 1991. Perilipin, a major hormonally regulated adipocyte-specific phosphoprotein associated with the periphery of lipid storage droplets. Journal of Biological Chemistry 266:11341–11346.

[14] Puri, V., Konda, S., Ranjit, S., Aouadi, M., Chawla, A., Chouinard, M., et al., 2007. Fat-specific protein 27, a novel lipid droplet protein that enhances triglyceride storage. Journal of Biological Chemistry 282:34213–34218.

[15] Gandotra, S., Le Dour, C., Bottomley, W., Cervera, P., Giral, P., Reznik, Y., et al., 2011. Perilipin deficiency and autosomal dominant partial lipodystrophy. New England Journal of Medicine 364:740–748.

[16] Rubio-Cabezas, O., Puri, V., Murano, I., Saudek, V., Semple, R.K., Dash, S., et al., 2009. Partial lipodystrophy and insulin resistant diabetes in a patient with a homozygous nonsense mutation in CIDEC. EMBO Molecular Medicine 1:280–287.

[17] Cannon, B., Nedergaard, J., 2004. Brown adipose tissue: function and physiological significance. Physiological Reviews 84:277–359.

[18] Himms-Hagen, J., 1984. Nonshivering thermogenesis. Brain Research Bulletin 12:151–160.

[19] Nedergaard, J., Bengtsson, T., Cannon, B., 2007. Unexpected evidence for active brown adipose tissue in adult humans. American Journal of Physiology. Endocrinology and Metabolism 293:E444–E452.

[20] Chondronikola, M., Volpi, E., Borsheim, E., Porter, C., Saraf, M.K., Annamalai, P., et al., 2016. Brown adipose tissue activation is linked to distinct systemic effects on lipid metabolism in humans. Cell Metabolism 23:1200–1206.

[21] Ouellet, V., Labbe, S.M., Blondin, D.P., Phoenix, S., Guerin, B., Haman, F., et al., 2012. Brown adipose tissue oxidative metabolism contributes to energy expenditure during acute cold exposure in humans. Journal of Clinical Investigation 122:545–552.

[22] Nedergaard, J., Cannon, B., 2014. The browning of white adipose tissue: some burning issues. Cell Metabolism 20:396–407.

[23] Maloney, S.K., Fuller, A., Mitchell, D., Gordon, C., Overton, J.M., 2014. Translating animal model research: does it matter that our rodents are cold? Physiology (Bethesda) 29:413–420.

[24] DiStefano, M.T., Danai, L.V., Roth Flach, R.J., Chawla, A., Pedersen, D.J., Guilherme, A., et al., 2015. The lipid droplet protein hypoxia-inducible gene 2 promotes hepatic triglyceride deposition by inhibiting lipolysis. Journal of Biological Chemistry 290:15175–15184.

[25] Folch, J., Lees, M., Sloane Stanley, G.H., 1957. A simple method for the isolation and purification of total lipides from animal tissues. Journal of Biological Chemistry 226:497–509.

[26] Hardy, O.T., Perugini, R.A., Nicoloro, S.M., Gallagher-Dorval, K., Puri, V., Straubhaar, J., et al., 2011. Body mass index-independent inflammation in omental adipose tissue associated with insulin resistance in morbid obesity. Surgery for Obesity and Related Diseases: Official Journal of the American Society for Bariatric Surgery 7:60–67.

[27] Jiang, Z.Y., Zhou, Q.L., Coleman, K.A., Chouinard, M., Boese, Q., Czech, M.P., 2003. Insulin signaling through Akt/protein kinase B analyzed by small interfering RNA-mediated gene silencing. Proceedings of the National Academy of Sciences of the United States of America 100:7569–7574.

[28] Wabitsch, M., Brenner, R.E., Melzner, I., Braun, M., Moller, P., Heinze, E., et al., 2001. Characterization of a human preadipocyte cell strain with high capacity for adipose differentiation. International Journal of Obesity and Related Metabolic Disorders 25:8–15.

[29] Greenberg, A.S., Egan, J.J., Wek, S.A., Moos Jr., M.C., Londos, C., Kimmel, A.R., 1993. Isolation of cDNAs for perilipins A and B: sequence and expression of lipid droplet-associated proteins of adipocytes. Proceedings of the National Academy of Sciences of the United States of America 90:12035–12039.

[30] Brasaemle, D.L., Barber, T., Wolins, N.E., Serrero, G., Blanchette-Mackie, E.J., Londos, C., 1997. Adipose differentiation-related protein is an ubiquitously expressed lipid storage droplet-associated protein. Journal of Lipid Research 38:2249–2263.

[31] Jiang, H.P., Harris, S.E., Serrero, G., 1992. Molecular cloning of a differentiation-related mRNA in the adipogenic cell line 1246. Cell Growth & Differentiation 3:21—30.

[32] Scherer, P.E., Bickel, P.E., Kotler, M., Lodish, H.F., 1998. Cloning of cell-specific secreted and surface proteins by subtractive antibody screening. Nature Biotechnology 16:581—586.

[33] Danesch, U., Hoeck, W., Ringold, G.M., 1992. Cloning and transcriptional regulation of a novel adipocyte-specific gene, FSP27. CAAT-enhancer-binding protein (C/EBP) and C/EBP-like proteins interact with sequences required for differentiation-dependent expression. Journal of Biological Chemistry 267: 7185—7193.

[34] Feldmann, H.M., Golozoubova, V., Cannon, B., Nedergaard, J., 2009. UCP1 ablation induces obesity and abolishes diet-induced thermogenesis in mice exempt from thermal stress by living at thermoneutrality. Cell Metabolism 9: 203—209.

[35] Abreu-Vieira, G., Fischer, A.W., Mattsson, C., de Jong, J.M., Shabalina, I.G., Ryden, M., et al., 2015. Cidea improves the metabolic profile through expansion of adipose tissue. Nature Communications 6:7433.

[36] Zhou, L., Park, S.Y., Xu, L., Xia, X., Ye, J., Su, L., et al., 2015. Insulin resistance and white adipose tissue inflammation are uncoupled in energetically challenged Fsp27-deficient mice. Nature Communications 6:5949.

[37] Zhou, Z., Yon Toh, S., Chen, Z., Guo, K., Ng, C.P., Ponniah, S., et al., 2003. Cidea-deficient mice have lean phenotype and are resistant to obesity. Nature Genetics 35:49—56.

[38] Ma, T., Lopez-Aguiar, A.G., Li, A., Lu, Y., Sekula, D., Nattie, E.E., et al., 2014. Mice lacking G0S2 are lean and cold-tolerant. Cancer Biology & Therapy 15: 643—650.

[39] McManaman, J.L., Bales, E.S., Orlicky, D.J., Jackman, M., MacLean, P.S., Cain, S., et al., 2013. Perilipin-2-null mice are protected against diet-induced obesity, adipose inflammation, and fatty liver disease. Journal of Lipid Research 54:1346—1359.

[40] Kuramoto, K., Okamura, T., Yamaguchi, T., Nakamura, T.Y., Wakabayashi, S., Morinaga, H., et al., 2012. Perilipin 5, a lipid droplet-binding protein, protects heart from oxidative burden by sequestering fatty acid from excessive oxidation. Journal of Biological Chemistry 287:23852—23863.

[41] Harms, M., Seale, P., 2013. Brown and beige fat: development, function and therapeutic potential. Nature Medicine 19:1252—1263.

[42] Lass, A., Zimmermann, R., Haemmerle, G., Riederer, M., Schoiswohl, G., Schweiger, M., et al., 2006. Adipose triglyceride lipase-mediated lipolysis of cellular fat stores is activated by CGI-58 and defective in Chanarin-Dorfman Syndrome. Cell Metabolism 3:309—319.

[43] Lord, C.C., Ferguson, D., Thomas, G., Brown, A.L., Schugar, R.C., Burrows, A., et al., 2016. Regulation of hepatic triacylglycerol metabolism by CGI-58 does not require ATGL Co-activation. Cell Reports 16:939—949.

[44] Villarroya, J., Cereijo, R., Villarroya, F., 2013. An endocrine role for brown adipose tissue? American Journal of Physiology. Endocrinology and Metabolism 305:E567—E572.

[45] Whittle, A.J., Carobbio, S., Martins, L., Slawik, M., Hondares, E., Vazquez, M.J., et al., 2012. BMP8B increases brown adipose tissue thermogenesis through both central and peripheral actions. Cell 149:871—885.

[46] Virtue, S., Feldmann, H., Christian, M., Tan, C.Y., Masoodi, M., Dale, M., et al., 2012. A new role for lipocalin prostaglandin d synthase in the regulation of brown adipose tissue substrate utilization. Diabetes 61:3139—3147.

[47] Rosell, M., Hondares, E., Iwamoto, S., Gonzalez, F.J., Wabitsch, M., Staels, B., et al., 2012. Peroxisome proliferator-activated receptors-alpha and -gamma, and cAMP-mediated pathways, control retinol-binding protein-4 gene expression in brown adipose tissue. Endocrinology 153:1162—1173.

[48] Hondares, E., Iglesias, R., Giralt, A., Gonzalez, F.J., Giralt, M., Mampel, T., et al., 2011. Thermogenic activation induces FGF21 expression and release in brown adipose tissue. Journal of Biological Chemistry 286:12983—12990.

[49] Gunawardana, S.C., Piston, D.W., 2012. Reversal of type 1 diabetes in mice by brown adipose tissue transplant. Diabetes 61:674—682.

[50] Kenny, P.A., Enver, T., Ashworth, A., 2005. Receptor and secreted targets of Wnt-1/beta-catenin signalling in mouse mammary epithelial cells. BMC Cancer 5:3.

[51] Gimm, T., Wiese, M., Teschemacher, B., Deggerich, A., Schodel, J., Knaup, K.X., et al., 2010. Hypoxia-inducible protein 2 is a novel lipid droplet protein and a specific target gene of hypoxia-inducible factor-1. FASEB Journal 24:4443—4458.

[52] Gandotra, S., Lim, K., Girousse, A., Saudek, V., O'Rahilly, S., Savage, D.B., 2011. Human frame shift mutations affecting the carboxyl terminus of perilipin increase lipolysis by failing to sequester the adipose triglyceride lipase (ATGL) coactivator AB-hydrolase-containing 5 (ABHD5). Journal of Biological Chemistry 286:34998—35006.

